MICROCOPY   CHART

TECHNICAL REPORT ARCCB-TR-86012

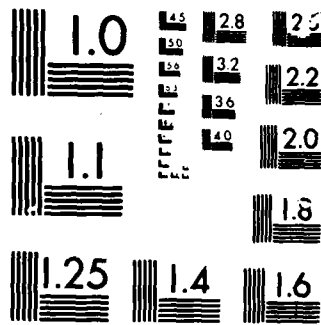# A NEW METHOD OF PREDICTING RESIDUAL

STRESSES IN AUTOFRETTAGED GUN BARRELS

AD-A167 633

P. C. T. CHEN

DTIC
ELECTE
S APR 30 1986
D
B

APRIL 1986

US ARMY ARMAMENT RESEARCH AND DEVELOPMENT CENTER
CLOSE COMBAT ARMAMENTS CENTER
BENÉT WEAPONS LABORATORY
WATERVLIET. N.Y. 12189-4050

86 4 28 218

DISCLAIMER

The findings in this report are not to be construed as an official

Department of the Army position unless so designated by other authorized

documents.

The use of trade name(s) and/or manufacturer(s) does not constitute

an official indorsement or approval.

DESTRUCTION NOTICE

For classified documents, follow the procedures in DoD 5200.22-M,

Industrial Security Manual, Section II-19 or DoD 5200.1-R, Information

Security Program Regulation, Chapter IX.

For unclassified, limited documents, destroy by any method that will

prevent disclosure of contents or reconstruction of the document.

For unclassified, unlimited documents, destroy when the report is

no longer needed. Do not return it to the originator.

REPORT DOCUMENTATION PAGE		READ INSTRUCTIONS BEFORE COMPLETING FORM
1. REPORT NUMBER ARCCB-TR-86012	2. GOVT ACCESSION NO. AD-A167633	3. RECIPIENT'S CATALOG NUMBER
4. TITLE (and Subtitle) A NEW METHOD OF PREDICTING RESIDUAL STRESSES IN AUTOFRETTAGED GUN BARRELS		5. TYPE OF REPORT & PERIOD COVERED Final
		6. PERFORMING ORG. REPORT NUMBER
7. AUTHOR(s) P. C. T. Chen		8. CONTRACT OR GRANT NUMBER(s)
9. PERFORMING ORGANIZATION NAME AND ADDRESS US Army Armament Research & Development Center Benet Weapons Laboratory, SMCAR-CCB-TL Watervliet, NY 12189-4050		10. PROGRAM ELEMENT, PROJECT, TASK AREA & WORK UNIT NUMBERS AMCMS No. 6111.02.H600.0 PRON No. 1A6DZ602NMSC
11. CONTROLLING OFFICE NAME AND ADDRESS US Army Armament Research & Development Center Close Combat Armaments Center Dover, NJ 07801-5001		12. REPORT DATE April 1986
		13. NUMBER OF PAGES 22
14. MONITORING AGENCY NAME & ADDRESS(if different from Controlling Office)		15. SECURITY CLASS. (of this report) UNCLASSIFIED
		15a. DECLASSIFICATION/DOWNGRADING SCHEDULE

16. DISTRIBUTION STATEMENT (of this Report)

Approved for public release; distribution unlimited.

17. DISTRIBUTION STATEMENT (of the abstract entered in Block 20, if different from Report)

18. SUPPLEMENTARY NOTES

To be presented at U.S. Army Science Conference, U.S. Military Academy, West Point, NY, 17-20 June 1986.
To be published in Proceedings of the Conference.

19. KEY WORDS (Continue on reverse side if necessary and identify by block number)

High Strength Steel	Strain-Hardening
Gun Barrel	Residual Stress
Bauschinger Effect	Autofrettage

20. ABSTRACT (Continue on reverse side if necessary and identify by block number)

The determination of residual stresses in autofrettaged gun barrels has been considered by many investigators using different mathematical methods and material models. Most of the earlier solutions were based on the assumption that the material behaves elastically on the release of the autofrettaged pressure. However, many materials, particularly the quenched and tempered, low alloy steels generally used for high pressure vessels, exhibit a significant

(CONT'D ON REVERSE)

DD FORM 1473 1 JAN 73 EDITION OF 1 NOV 65 IS OBSOLETE

20. ABSTRACT (CONT'D)

Bauschinger effect. In a recent paper, this author presented a closed-form solution of residual stresses in autofrettaged tubes based on a theoretical model considering the Bauschinger and hardening effects during unloading, but neglecting the strain-hardening during loading. A more general theoretical model without this restriction was proposed earlier, but only part of the final results were shown. In the present report, the complete method of stress and deformation analysis based on the general theoretical model is stated. The new model is a better representation of the actual loading/ unloading behavior in a high strength steel. The Bauschinger effect factor is treated as a function of overstrain. The strain-hardening effect is taken into account with different parameters used for loading and unloading processes. The formulas for calculating stresses, strains, and displacements are given. The new results indicate that the influence of the Bauschinger and hardening effects on residual stresses is significant. A comparison with two experimental results has been made.

Accession For

NTIS GRA&I
DTIC TAB
Unannounced
Justification

By
Distribution/

Availability Codes

Dist   Avail and/or
        Special

A-1

DTIC
ELECTE
APR 30 1986
B

TABLE OF CONTENTS

LIST OF ILLUSTRATIONS

i

ACKNOWLEDGEMENTS

ii

INTRODUCTION

A thick-walled cylinder is used for a variety of applications in the chemical, nuclear, and armament industries where large internal pressures have to be withstood. In the absence of residual stresses, the cracks usually form at the bore where the hoop stress developed by the pressure is highest. To prevent such failure and to increase the pressure-carrying capacity, a common practice is autofrettage treatment of the cylinder prior to use (ref 1). This process has the effect of producing beneficial compressive residual hoop stresses near the bore which can prolong the fatigue life.

The determination of residual stresses in autofrettaged cylinders has been considered by many investigators using different mathematical methods and material models (refs 2-8). Most of the earlier solutions were based on the assumption that the material behaves elastically on the release of the autofrettage pressure. However, many materials, particularly the quenched and tempered, low alloy steels generally used for high pressure vessels, exhibit a significant Bauschinger effect (ref 9). In a recent paper (ref 10), this author presented a closed-form solution of residual stresses in autofrettaged tubes based on a theoretical model considering the Bauschinger and hardening effects during unloading, but neglecting the strain-hardening effects during loading. A more general theoretical model without this restriction was proposed earlier, but only part of the final results were shown due to space limitation (ref 11). In the present report, the complete method of stress and deformation analysis based on the general theoretical model is stated. The new model is a better representation of the actual loading/unloading behavior

References are listed at the end of this report.

1

in a high strength steel. The Bauschinger effect factor is treated as a function of overstrain. The strain-hardening effect is taken into account with different parameters used for loading and unloading processes. The formulas for calculating stresses, strains, and displacements are given and new results of residual stresses in autofrettaged high pressure vesssels are presented.

MATERIAL BEHAVIOR AND MODELING

The material chosen for this investigation was a modified 4330 steel having a martensitic structure. A description of its chemical composition and various heat treatments is given in Reference 9 by Milligan, Koo, and Davidson. They studied behavior by utilizing a uniaxial tension-compression specimen. Figure 1 shows the stress-strain curve during loading and unloading after overstrains in tension. The stress-strain curve during loading can be replaced with sufficient accuracy by a bilinear elastic-plastic model shown in the figure by the broken lines. For the plastic portion, the yield stress (σ) is related to the plastic strain (ϵ^p) by

$$\sigma/\sigma_0 = 1 + m\zeta/(1-m) \quad \text{and} \quad \zeta = (E/\sigma_0)\epsilon^p \tag{1}$$

where Young's modulus (E), tangent modulus (mE), initial yield stress (σ_0), and the Poisson's ratio (ν) are the material constants. The nominal yield strength at 0.1 percent offset was chosen as the initial yield stress.

Initially, the yield stresses in tension and compression are approximately equal so that the material can be considered as isotropic. However, the ratio of the yield stress upon reverse yielding to the initial yield stress is strongly affected by overstrain in a high strength steel. The values of the Bauschinger effect factor (BEF) also depend on the 0.1 percent offset mentioned above. Taking into account strain-hardening, the definition of the BEF is

2

$$BEF = (\sigma_0{}' - \sigma_1)(/\sigma_1 = f(\epsilon_1{}^p) \qquad\qquad (2)$$

where σ_1, $\epsilon_1{}^p$ are the yield stress, plastic strain just before unloading occurs, and $\sigma_0{}'$ is the linear drop in stress until reverse yielding begins. Figure 2 shows the Bauschinger effect factor (f) as a function of percent tensile overstrain (c^p). The graph shows a decrease of the BEF with increasing amount of tensile prestrain up to approximately two percent at which point it becomes effectively constant.

In most of the plasticity theories, the curve of reverse loading is uniquely defined by the curve of the first loading. The present model does not assume such a relationship. The experimental stress-strain curve during unloading is used directly. A piecewise linear representation can be used, but only a bilinear approximation was chosen here as shown in Figure 1. In the same figure, we also show two other theoretical models in dotted lines for this material subjected to unloading with further plastic flow. They are isotropic and kinematic hardening models. A summary of the plasticity theories given by Armen (ref 12) illustrates the fact that all of the theories are capable of treating the monotonic loading situation. For cyclic loading, including reverse yielding, kinematic and isotropic hardening represent the limits to the actual behavior, whereas the remaining theories are falling anywhere within these limits. The above conclusion indicates that none of the existing models can accurately represent the actual material behavior as shown in Figure 1. The reverse yielding begins at a stress whose magnitude is smaller than that predicted by all existing theories and the slope of strain-hardening after reverse yielding is much larger than that during the first loading process. The new bilinear model presented here is a better approximation to the actual material behavior.
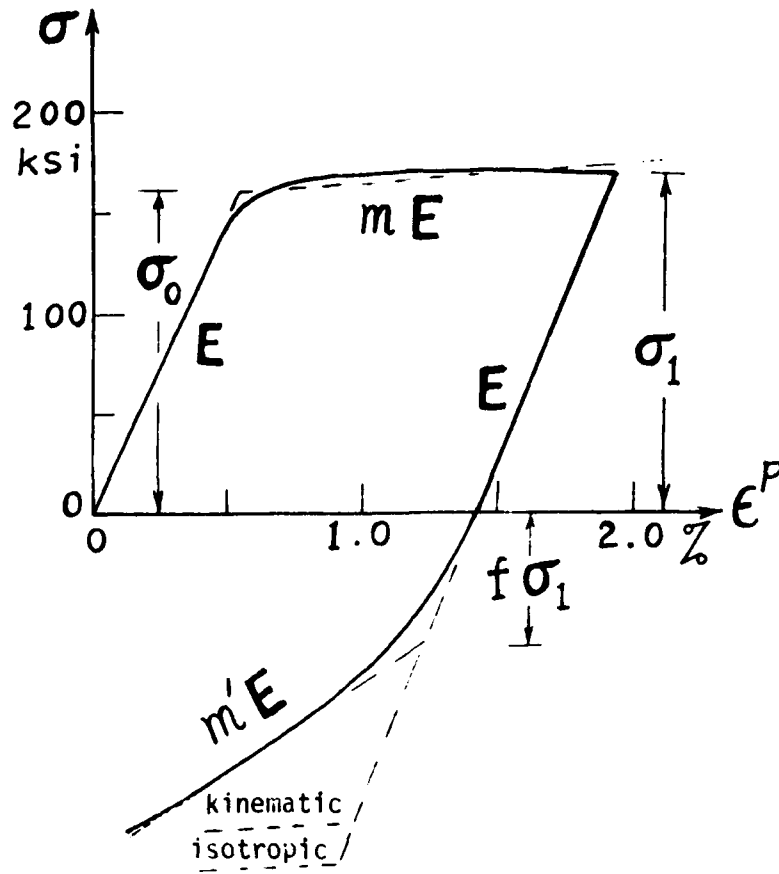
Figure 1.   Stress-strain curve during loading and unloading.

Choosing a new coordinate system (σ', ϵ') with the origin at the point before unloading, we have for the plastic portion of the reverse yielding curve

$$\sigma'/\sigma_0 = \sigma_0'/\sigma_0 + m'\zeta'/(1-m') \quad \text{and} \quad \zeta' = (E/\sigma_0)\epsilon'^p \tag{3}$$

where $m'E$ is the slope of the reverse yielding curve and ϵ'^p is the additional plastic strain during unloading. According to Eqs. (1) and (2), σ_0' can be expressed as a function of plastic strain (ϵ_1^p) just prior to unloading by

$$\sigma_0'/\sigma_0 = [1 + m\zeta_1/(1-m)][1 + f(\zeta_1)] = g(\zeta_1) \tag{4}$$

4

With experimental data $f(\epsilon^p)$ shown in Figure 2, we can calculate σ_0' and determine the initiation of reverse yielding. The slope of reverse yielding (m'E) could be expressed also as a function of prestrain (ϵ^p and ϵ'^p) if more experimental unloading curves were available. Based on limited information, the slope of reverse yielding (m'E) is estimated to be in the range of (9.4 to 8.3) x 10⁶ psi. It seems that this slope is not very sensitive to prestrain and a constant value, say m' = 0.3, may be assumed.
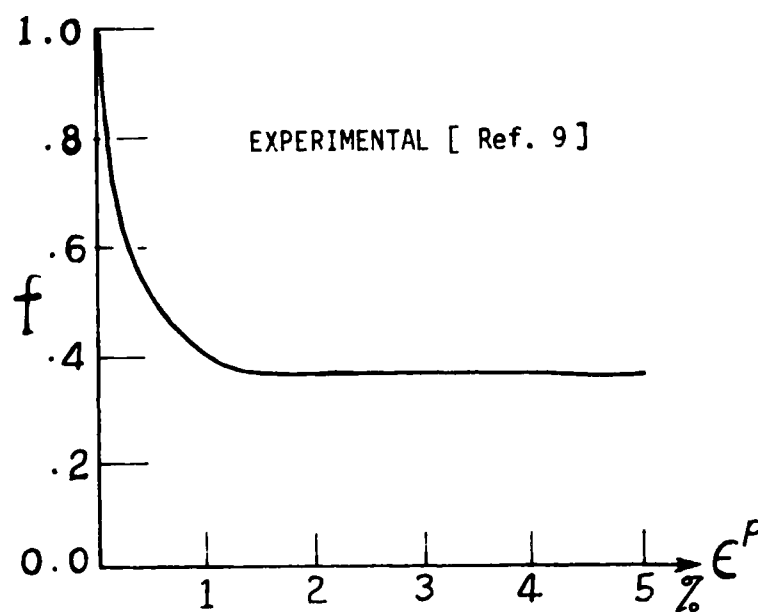
Figure 2. Bauschinger effect factor as a function of overstrain.

ELASTIC-PLASTIC LOADING

Consider a thick-walled cylinder, internal radius a and external radius b, which is subjected to internal pressure p. The material is assumed to be elastic-plastic, obeying the Tresca's yield criterion, the associated flow theory, and a linear strain-hardening rule. The elastic-plastic solution during loading has been found by Bland (ref 3). The expressions for the radial and hoop stresses are:

5

$$\begin{array}{ll}
\sigma_r/\sigma_0 \\
\sigma_\theta/\sigma_0
\end{array} = \frac{1}{2}\left(\mp 1 + \frac{\rho^2}{b^2}\right) \mp \frac{1}{2}\beta_2\left(\frac{\rho^2}{r^2} - 1\right) - (1-\beta_2)\log\frac{\rho}{r} \quad \text{for } a \leqslant r \leqslant \rho \quad \begin{array}{l}(5)\\[1em](6)\end{array}$$

subject to $\sigma_\theta \geqslant \sigma_z \geqslant \sigma_r$

$$\begin{array}{ll}
\sigma_r/\sigma_0 \\
\sigma_\theta/\sigma_0
\end{array} = \frac{1}{2}\left(\frac{\rho^2}{b^2} \mp \frac{\rho^2}{r^2}\right) \quad \text{for } \rho \leqslant r \leqslant b \quad \begin{array}{l}(7)\\[1em](8)\end{array}$$

$$\sigma_z/\sigma_0 = \nu(\sigma_r+\sigma_\theta)/\sigma_0 + E\epsilon_z/\sigma_0 \tag{9}$$

$$\frac{E}{\sigma_0}\frac{u}{r} = (1-2\nu)(1+\nu)\frac{\sigma_r}{\sigma_0} + (1-\nu^2)\frac{\rho^2}{r^2} - \nu\frac{E}{\sigma_0}\epsilon_z \tag{10}$$

and

$$(E/\sigma_0)\epsilon_z = \frac{(\mu-2\nu)}{b^2/a^2-1}(P/\sigma_0) \tag{11}$$

where $\mu = 0$ (open-end), 1 (closed-end), and ρ is the elastic-plastic boundary relating to the internal pressure p by

$$p/\sigma_0 = \frac{1}{2}(1-\rho^2/b^2) + (1-\beta_2)\log(\rho/a) + \frac{1}{2}\beta_2(\rho^2/a^2-1) \tag{12}$$

The equivalent plastic strain can be calculated by

$$(E/\sigma_0)\epsilon^p = \zeta = \beta_1(\rho^2/r^2-1) \quad, \quad \text{in } (a \leqslant r \leqslant \rho) \tag{13}$$

and

$$\beta_1 = \frac{1-m}{m + \dfrac{\sqrt{3}}{2}\dfrac{(1-m)}{(1-\nu^2)}} \quad, \quad \beta_2 = m\beta_1/(1-m) \tag{14}$$

REVERSE YIELDING

If the pressure p given by Eq. (12) is subsequently removed completely with no reverse yielding, the unloading is entirely elastic and the solution is given by

$$\begin{matrix} \sigma_r' \\ \sigma_\theta' \end{matrix} = \frac{p}{b^2/a^2-1} \left[\mp \frac{b^2}{r^2} - 1 \right]$$

<div style="text-align:right">(15)
(16)</div>

$$\sigma_z' = \nu(\sigma_r' + \sigma_\theta') + E\epsilon_z' \tag{17}$$

$$E\epsilon_z' = -(\mu-2\nu)p/(b^2/a^2-1) \tag{18}$$

$$Eu'/r = -[(1-\nu-\mu\nu) + (1+\nu)b^2/r^2]p/(b^2/a^2-1) \tag{19}$$

Let a double prime denote a component in the residual state, i.e., $\sigma_\theta'' = \sigma_\theta + \sigma_\theta'$. Assuming a reduced compressive yield strength as a result of the Bauschinger effect and using Tresca's yield criterion subject to $\sigma_r'' > \sigma_z'' > \sigma_\theta''$, the reverse yielding will not occur if

$$\sigma_r'' - \sigma_\theta'' \leqslant \sigma'' = f\sigma_0[1 + m\zeta/(1-m)] \tag{20}$$

Substituting the loading and unloading solutions into Eq. (20), we can determine the minimum pressure (p_m) for reverse yielding to occur. The equation for p_m is given by

$$p_m/\sigma_0 = \frac{1}{2}(1-a^2/b^2)[1 + m\zeta_m/(1-m)][1 + f(\zeta_m)] \tag{21}$$

and $\zeta_m = \beta_1(\rho_m^2/a^2-1)$.

Equating Eqs. (12) to (21), we can determine the minimum amount of overstrain (ρ_m) and calculate the minimum pressure (p_m) required for reverse yielding.

ELASTIC-PLASTIC UNLOADING

Now suppose that the loading has been such that the internal pressure is larger than p_m given by Eq. (21). On unloading, yielding will occur for $a \leqslant r \leqslant \rho'$ with $\rho' > \rho$. In the reverse yielding zone, the stresses in the residual state satisfy

$$\sigma_r'' - \sigma_\theta'' = \sigma'' \tag{22}$$

7

assuming that $\sigma_r" \geqslant \sigma_z" \geqslant \sigma_\theta"$. Since the yield criterion during loading is

$$\sigma_\theta - \sigma_r = \sigma \tag{23}$$

we have

$$\sigma_r' - \sigma_\theta' = (\sigma_r" - \sigma_\theta") + (\sigma_\theta - \sigma_r) = \sigma" + \sigma = \sigma' \tag{24}$$

where σ and σ' are defined by Eqs. (1) and (3), respectively.

The material is assumed to obey the associated flow theory and a linear strain-hardening rule during unloading. Following the procedure in Bland's work (ref 3), an analytical solution for elastic-plastic unloading can be found. The stresses in the reverse yielding zone ($a \leqslant r \leqslant \rho'$) are given by

$$\sigma_r'/\sigma_O = P/\sigma_O - \Gamma(\zeta_r, \zeta_a) \tag{25}$$

$$\sigma_\theta'/\sigma_O = \sigma_r'/\sigma_O - g(\zeta) - m'\zeta'/(1-m') \tag{26}$$

$$\zeta' = \beta_1[g(\zeta_\rho')\rho'^2/r^2 - g(\zeta)] \tag{27}$$

where

$$\beta_1' = (1-m')/[m' + \frac{\sqrt{3}}{2} \frac{(1-m')}{(1-\nu^2)}] \quad , \quad \beta_2' = m'\beta_2'/(1-m') \tag{28}$$

$$\Gamma(\zeta_r, \zeta_a) = -\frac{1}{2}(\beta_2'/\beta_1)(\rho'/\rho)^2(\zeta_r - \zeta_a)g(\zeta_\rho') + (1-\beta_2')G(\zeta_r, \zeta_a) \tag{29}$$

$$G(\zeta_r, \zeta_a) = \int_{\zeta_r}^{\zeta_a} \frac{1}{2}(\zeta + \beta_1)^{-1}g(\zeta)d\zeta \tag{30}$$

$g(\zeta)$ is given by Eq. (4) and ζ_r, ζ_a can be calculated by Eq. (12). For some special cases, e.g. Reference (10), explicit expressions for $G(\zeta_r, \zeta_a)$ can be obtained. In general, numerical integration is needed.

The stresses in the elastic zone ($\rho' \leqslant r \leqslant b$) are

$$\begin{matrix} \sigma_r'/\sigma_O \\ \\ \sigma_\theta'/\sigma_O \end{matrix} = \frac{1}{2}g(\zeta_\rho')[\pm(\rho'/r)^2 - (\rho'/b)^2] \quad \begin{matrix} (31) \\ \\ (32) \end{matrix}$$

The location of the reverse yielding zone can be found by the continuity of σ_r' at ρ' from Eqs. (25) and (31).

The other expressions in the entire tube (a $\leqslant$ r $\leqslant$ b) are

$$\sigma_z'/\sigma_0 = \nu(\sigma_r'+\sigma_\theta')/\sigma_0 + E\epsilon_z'/\sigma_0 \qquad (33)$$

$$E\epsilon_z'/\sigma_0 = -(\mu-2\nu)(P/\sigma_0)/(b^2/a^2-1) \qquad (34)$$

$$(E/\sigma_0)u'/r = (1-2\nu)(1+\nu)(\sigma_r'/\sigma_0) - \nu E\epsilon_z'/\sigma_0$$
$$- (1-\nu^2)(\rho'/r)^2 g(\zeta_\rho') \qquad (35)$$

The residual stresses and the residual displacement are found by addition

$$\sigma_r'' = \sigma_r + \sigma_r' \quad , \quad \sigma_\theta'' = \sigma_\theta + \sigma_\theta' \quad , \quad \sigma_z'' = \sigma_z + \sigma_z'$$

and

$$u'' = u + u' \qquad (36)$$

NUMERICAL RESULTS AND DISCUSSION

The numerical results for three closed-end thick-walled cylinders with various wall ratios have been obtained. The material constants in all cases were $\nu = 0.3$, $E/\sigma_0 = 200$, and m = 0.01. The Bauschinger effect factor (f) was determined during computations based on the experimental curve $f(\epsilon^p)$ as shown in Figure 8 of Reference 9. The slope of unloading after reverse yielding was estimated to be m' = 0.3 for a high strength steel. The computations for the stresses, strains, and displacements during elastic-plastic loading and after complete unloading were made, and some of the numerical results are presented graphically in Figures 3 through 10.

Figure 3 shows the relation between the pressure factor and the dimensionless elastic-plastic boundary for three closed-end tubes. The values of the pressure factor to reach 100 percent overstrain are 0.543, 0.702, 0.891 for b/a = 1.6, 2.0, 2.4, respectively. When the applied pressure in a

partially plastic tube is removed, residual displacements and stresses will occur. Figure 4 shows the residual displacements at the bore as functions of the elastic-plastic interface for wall ratios 1.6, 2.0, and 2.4. By combining the graphical results shown in Figures 3 and 4, we can obtain the functional relationship between the applied pressure and the residual displacement at the bore. The new results for the residual displacement shown in the figure are a little smaller than the well-known results based on the complete elastic unloading or the isotropic hardening material.
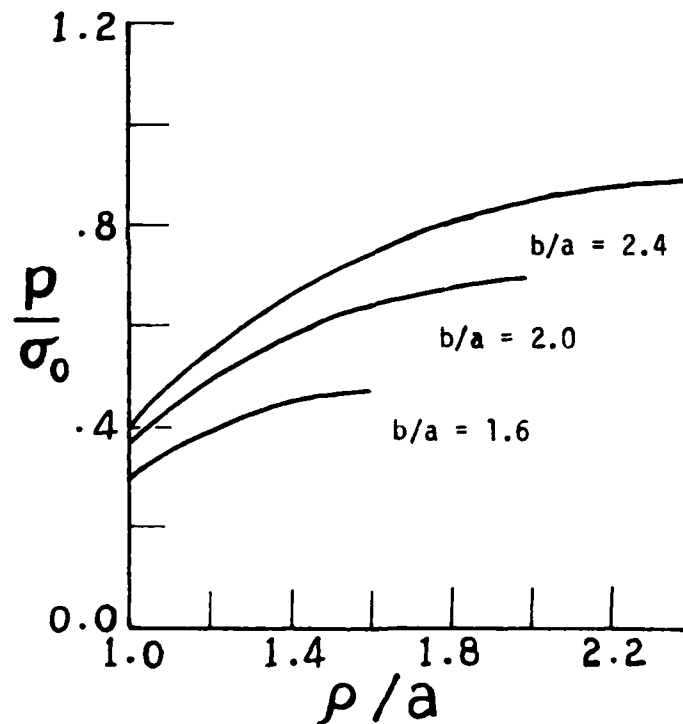

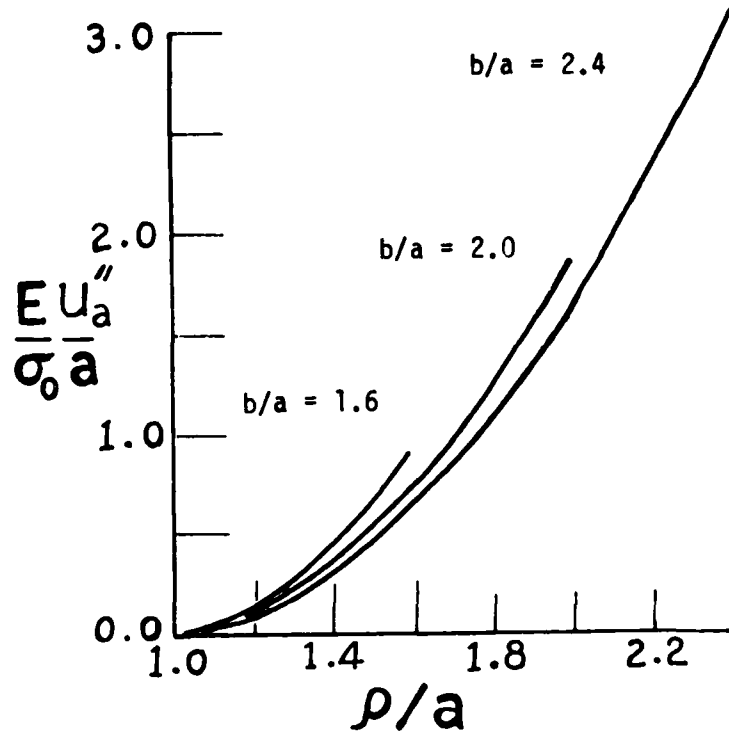Figure 3.   Internal pressure vs. elastic-plastic interface.

Figure 4. Residual displacement vs. elastic-plastic interface.

The numerical results for all stress components during loading and after unloading have been obtained for tubes with various wall ratios. Since the radial and axial stresses are not as important as the hoop stress, only the results for the latter are presented. Figure 5 shows the distribution of hoop stresses before and after unloading in a closed-end tube of wall ratio 1.6 corresponding to 0 percent, 50 percent, 100 percent overstrain, i.e., ρ/a = 1.0, 1.3, 1.6, respectively. Reverse yielding will not occur if $p/\sigma_0 < 0.46$ or $\rho/a < 1.429$. For a 100 percent overstrain, reverse yielding occurs in a small region, $a \leqslant r \leqslant 1.03a$, and the residual hoop stress at the bore is $-0.474\ \sigma_0$, instead of $-0.537\ \sigma_0$ based on elastic unloading. Figure 6 shows the residual stress distributions in an autofrettaged tube of wall ratio 2.0

11

for ρ/a = 1.2, 1.6, and 2.0. Reverse yielding will not occur if p/σ_0 < 0.583 or ρ/a = 1.373. When the pressure to reach 100 percent overstrain has been removed completely, reverse yielding occurs in $a \leqslant r \leqslant 1.173a$ and the residual hoop stress at the bore is $-0.377 \sigma_0$. Additional results of residual hoop stresses are shown in Figure 7 for an autofrettaged tube of wall ratio 2.4 with ρ/a = 1.2, 1.6, 2.0, and 2.4. Reverse yielding will not occur if p/σ_0 < 0.647 or ρ/a < 1.358. After complete unloading from 100 percent overstrain, reverse yielding occurs in $a \leqslant r \leqslant 1.315a$ and the residual hoop stress at the bore is $-0.389 \sigma_0$. As can be seen in Figures 6 and 7, the reverse yielding zone becomes larger as the amount of overstrain increases.
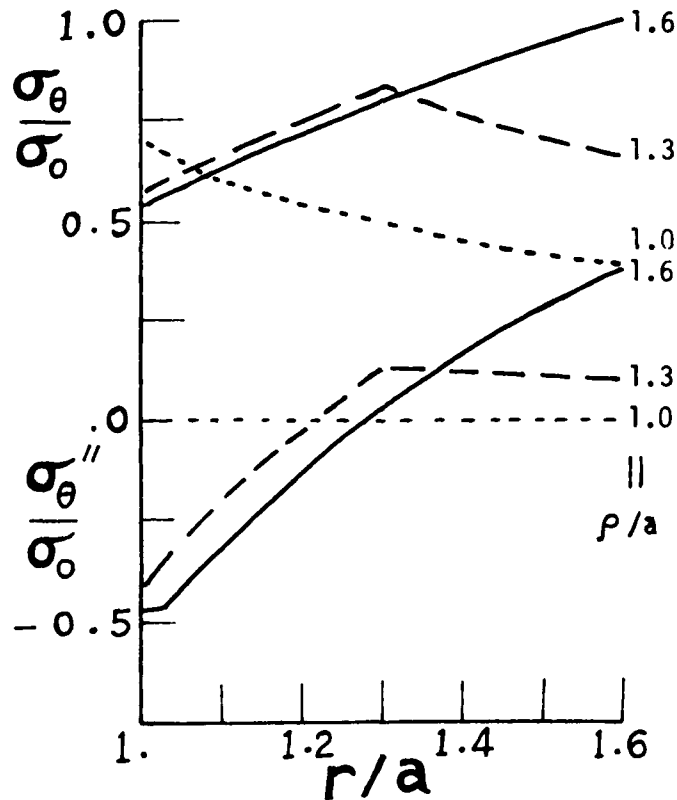

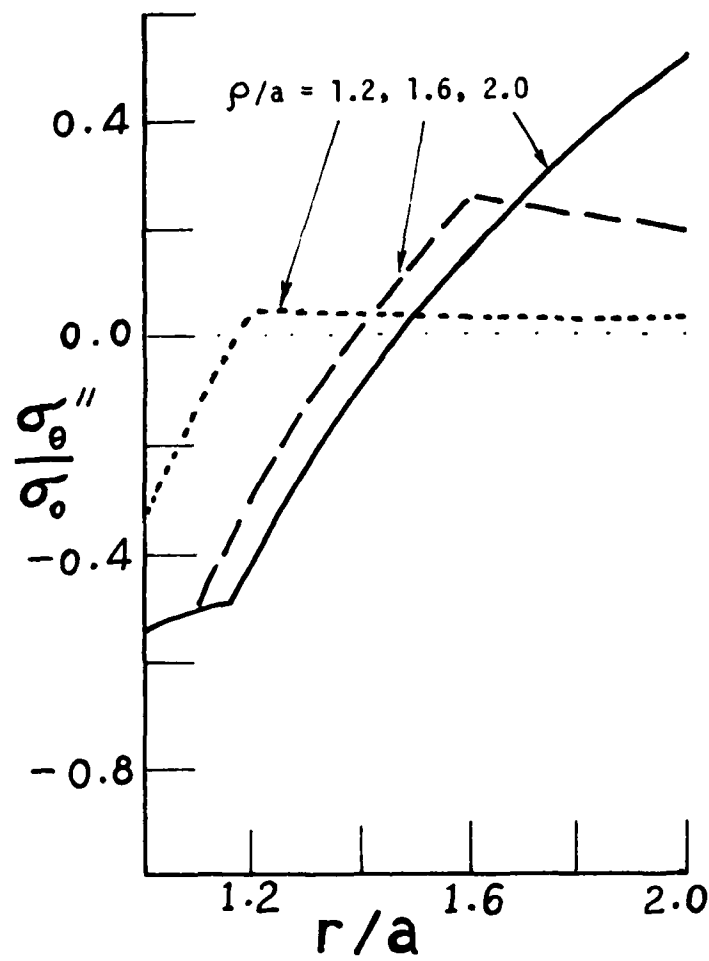Figure 5. Stress distribution before and after unloading in a tube with b/a = 1.6.

12

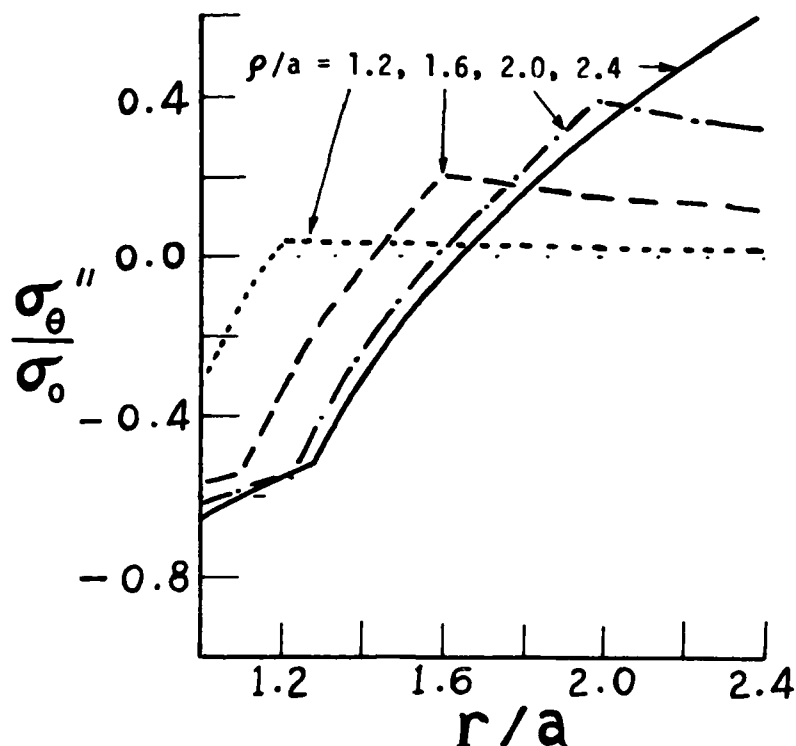Figure 6. Residual stress distribution in an autofrettaged tube with b/a = 2.0.

Figure 7. Residual stress distribution in an autofrettaged tube
with b/a = 2.4.

It is of interest to compare the new results for residual hoop stresses
with those based on the other theoretical models. Figure 8 shows a comparison
of residual hoop stresses based on three theoretical models for an auto-
frettaged tube of b/a = ρ/a = 2.0. The dotted line represents the well-known
solution based on the assumption of complete elastic unloading. The same
solution is obtained when either the isotropic or the kinematic hardening
model is used. The broken line represents the solution based on a model
including the Bauschinger effect but with the same hardening parameter m' = m
= 0.01. This solution is close to Parker's solution neglecting hardening com-
petely with m' = m = 0 (ref 8). As can be seen from this figure, the new
result represented by the solid line is quite different from the other two
solutions. This comparison also demonstrates that the Bauschinger effect and

14

strain-hardening during loading and unloading can have a significant effect on the residual stresses, especially near the bore.
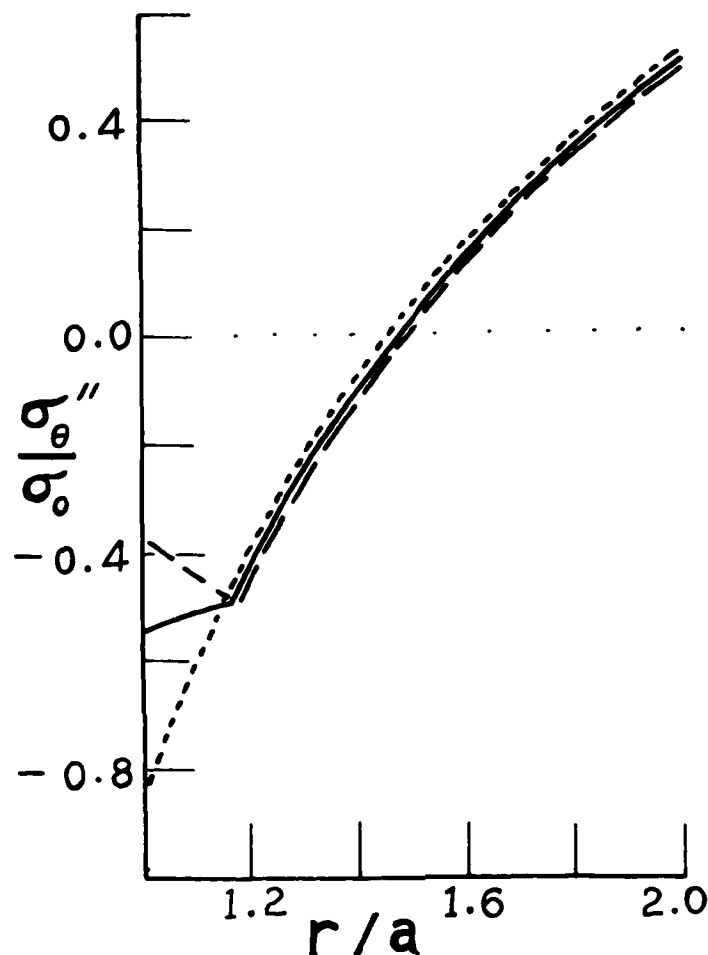
Figure 8. A comparison of three theoretical predictions (b = ρ = 2a).

For a closed-end tube of wall ratio 2.4 subjected to 100 percent overstrain, we show the comparison of residual hoop stresses based on three models in Figure 9. The dotted lines represent the solutions based on the isotropic hardening model (ref 3). Reverse yielding occurs even if the Bauschinger effect is neglected. The solid and broken lines represent the new model and the model with m' = m, respectively. As can be seen from these figures, the numerical results of the residual hoop stresses based on three

models are quite different in the reverse yielding zone. The new result is considered more accurate for our problem because it is based on a more general theoretical model considering the Bauschinger and hardening effects during loading and unloading.
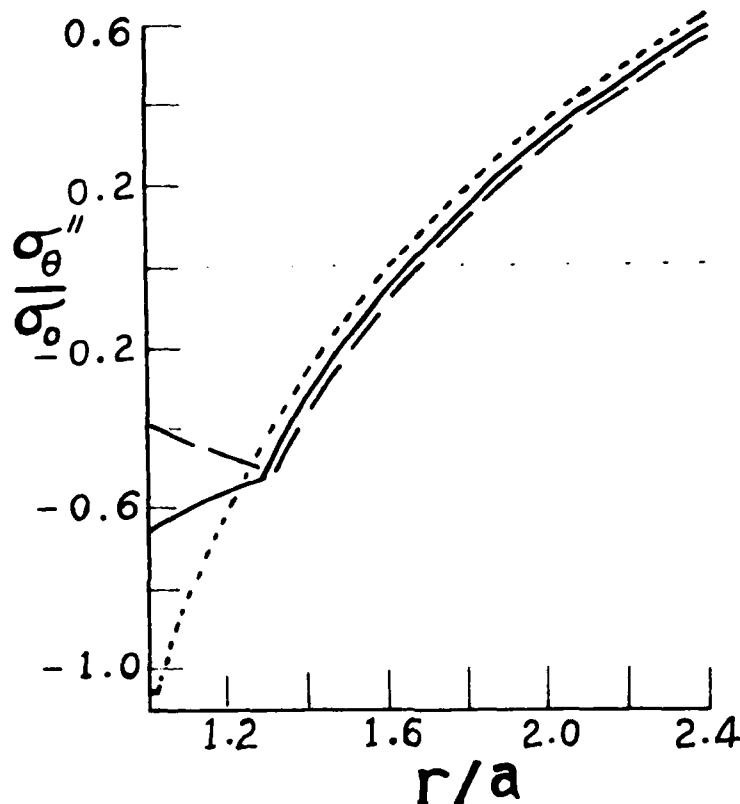
Figure 9. A comparison of three theoretical predictions (b = ρ = 2.4a).

In order to check the new theoretical prediction of residual stresses, a search of available experimental results has been made. Figure 10 shows a comparison with the results based on the x-ray method (ref 13) and the ultra-sonic method (ref 14) for a 155 mm autofrettaged gun tube. A good agreement has been reached in this comparison. The information on the residual stress distribution has been used in calculating the stress intensity factors (ref

15) and predicting the fatigue life of gun barrels (ref 16). These results will be published in the near future.
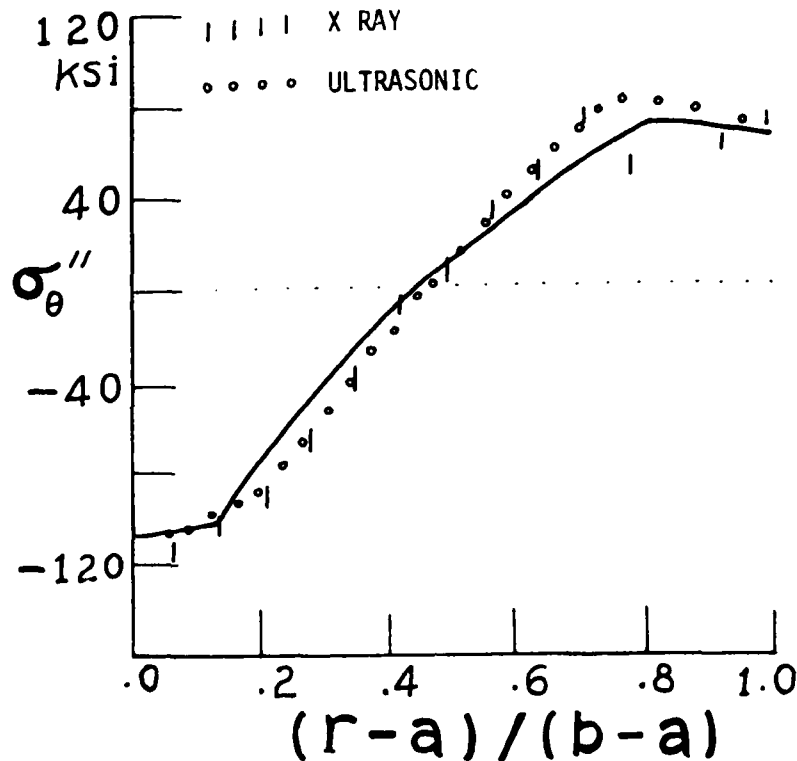
Figure 10. A comparison of theoretical prediction and experimental measurements in a 155 mm autofrettaged gun tube.

CONCLUSIONS

A new theoretical model for the high strength gun steel has been proposed. The real Bauschinger effect factor has been used to determine the range of elastic unloading. Different rates of strain-hardening during loading and unloading have been taken into account.

A new analytical solution for calculating the residual stresses and strains with reversed yielding has been obtained. The numerical results for the residual stress distributions in three autofrettaged gun tubes have been

17

given. The new results indicate that the influence of the Bauschinger and hardening effects on the residual stresses is significant.

A good agreement with two experimental results for a 155 mm autofrettaged gun tube has been reached. The new method is reliable, efficient, and economical. The new results have great implication to the fatigue life estimation of gun barrels.

REFERENCES

1. Davidson, T. E. and Kendall, D. P., "The Design of Pressure Vessels for Very High Pressure Operation," Mechanical Behavior of Materials Under Pressure, (H. L. P. Pugh, ed.), Elsevier Co., 1970.

2. Hill, R., The Mathematical Theory of Plasticity, Oxford University Press, London, 1950.

3. Bland, D. R., "Elastoplastic Thick-Walled Tubes of Work-Hardening Materials Subject to Internal and External Pressures and Temperature Gradients," Journal of Mechanics and Physics of Solids, Vol. 4, 1956, pp. 209-229.

4. Franklin, G. J. and Morrison, J. L. M., "Autofrettage of Cylinders: Prediction of Pressure/External Expansion Curves and Calculation of Residual Stresses," Proceedings of the Institute of Mechanical Engineers, Vol. 174, 1960, pp. 947-974.

5. Chen, P. C. T., "The Finite Element Analysis of Elastic-Plastic Thick-Walled Tubes," Proceedings of Army Symposium on Solid Mechanics, The Role of Mechanics in Design-Ballistic Problems, 1972, pp. 243-253.

6. Chen, P. C. T., "A Comparison of Flow and Deformation Theories in a Radially Stressed Annular Plate," Journal of Applied Mechanics, Vol. 40, 1973, pp. 283-287.

7. Chen, P. C. T., "Numerical Prediction of Residual Stresses in an Autofrettaged Tube of Compressible Material," Proceedings of the 1981 Army Numerical Analysis and Computer Conference, pp. 351-362.

8. Parker, A. P. and Andrasic, C. P., "Safe Life Design of Gun Tubes - Some Numerical Methods and Results," Proceedings of the 1981 Army Numerical Analysis and Computer Conference, pp. 311-333.

9. Milligan, R. V., Koo, W. H., and Davidson, T. E., "The Bauschinger
   Effect in a High Strength Steel," Journal of Basic Engineering, Vol. 88,
   June 1966, pp. 480-488.

10. Chen, P. C. T., "The Bauschinger and Hardening Effect on Residual
    Stresses in an Autofrettaged Thick-Walled Cylinder," Journal of Pressure
    Vessel Technology, Vol. 108, February 1986, pp. 108-112.

11. Chen, P. C. T., "Prediction of Residual Stresses in an Autofrettaged
    Thick-Walled Cylinder," Materials Research Society Symposium Proceedings,
    Vol. 22, 1984, pp. 235-238.

12. Armen, H., "Plasticity in General Software," Workshop on Inelastic
    Constitutive Equations for Metals, (E. Krempl, C. H. Wells, and Z.
    Zudans, eds.), Rensselaer Polytechnic Institute, Troy, NY, 1975, pp.
    56-78.

13. Capsimalis, G. P., Haggerty, R. F., and Loomis, K., "Computer Controlled
    X-Ray Stress Analysis for Inspection of Manufactured Components," WVT-TR-
    7701, Watervliet Arsenal, Watervliet, NY, January 1977.

14. Frankel, J., Scholz, W., Capsimalis, G. P., and Korman, W., "Residual
    Stress Measurement in Circular Steel Cylinder," ARLCB-TR-84018, Benet
    Weapons Laboratory, Watervliet, NY, May 1984.

15. Pu, S. L. and Chen, P. C. T., "The Bauschinger Effect on Stress Intensity
    Factors for a Radially Cracked Gun Tube," Transactions of the Third Army
    Conference on Applied Mathematics and Computing (In Press).

16. Pu, S. L. and Chen, P. C. T., "On Fatigue Life Prediction in Thick-Walled
    Cylinders," submitted to ASTM Symposium on Analytical and Experimental
    Methods for Residual Stress Effects in Fatigue to be held in October
    1986.

TECHNICAL REPORT INTERNAL DISTRIBUTION LIST

	NO. OF COPIES
CHIEF, DEVELOPMENT ENGINEERING BRANCH	
ATTN: SMCAR-CCB-D	1
-DA	1
-DP	1
-DR	1
-DS (SYSTEMS)	1
-DC	1
-DM	1
CHIEF, ENGINEERING SUPPORT BRANCH	
ATTN: SMCAR-CCB-S	1
-SE	1
CHIEF, RESEARCH BRANCH	
ATTN: SMCAR-CCB-R	2
-R (ELLEN FOGARTY)	1
-RA	1
-RM	1
-RP	1
-RT	1
TECHNICAL LIBRARY	5
ATTN: SMCAR-CCB-TL	
TECHNICAL PUBLICATIONS & EDITING UNIT	2
ATTN: SMCAR-CCB-TL	
DIRECTOR, OPERATIONS DIRECTORATE	1
DIRECTOR, PROCUREMENT DIRECTORATE	1
DIRECTOR, PRODUCT ASSURANCE DIRECTORATE	1

NOTE: PLEASE NOTIFY DIRECTOR, BENET WEAPONS LABORATORY, ATTN: SMCAR-CCB-TL, OF ANY ADDRESS CHANGES.

TECHNICAL REPORT EXTERNAL DISTRIBUTION LIST

	NO. OF COPIES		NO. OF COPIES
ASST SEC OF THE ARMY RESEARCH & DEVELOPMENT ATTN: DEP FOR SCI & TECH THE PENTAGON WASHINGTON, D.C. 20315	1	COMMANDER US ARMY AMCCOM ATTN: SMCAR-ESP-L ROCK ISLAND, IL 61299	1
COMMANDER DEFENSE TECHNICAL INFO CENTER ATTN: DTIC-DDA CAMERON STATION ALEXANDRIA, VA 22314	12	COMMANDER ROCK ISLAND ARSENAL ATTN: SMCRI-ENM (MAT SCI DIV) ROCK ISLAND, IL 61299	1
COMMANDER US ARMY MAT DEV & READ COMD ATTN: DRCDE-SG 5001 EISENHOWER AVE ALEXANDRIA, VA 22333	1	DIRECTOR US ARMY INDUSTRIAL BASE ENG ACTV ATTN: DRXIB-M ROCK ISLAND, IL 61299	1
COMMANDER ARMAMENT RES & DEV CTR US ARMY AMCCOM		COMMANDER US ARMY TANK-AUTMV R&D COMD ATTN: TECH LIB - DRSTA-TSL WARREN, MI 48090	1
ATTN: SMCAR-FS SMCAR-FSA SMCAR-FSM SMCAR-FSS SMCAR-AEE SMCAR-AES SMCAR-AET-O (PLASTECH) SMCAR-MSI (STINFO) DOVER, NJ 07801	1 1 1 1 1 1 1 2	COMMANDER US ARMY TANK-AUTMV COMD ATTN: DRSTA-RC WARREN, MI 48090 COMMANDER US MILITARY ACADEMY ATTN: CHMN, MECH ENGR DEPT WEST POINT, NY 10996	1 1
DIRECTOR BALLISTICS RESEARCH LABORATORY ATTN: AMXBR-TSB-S (STINFO) ABERDEEN PROVING GROUND, MD 21005	1	US ARMY MISSILE COMD REDSTONE SCIENTIFIC INFO CTR ATTN: DOCUMENTS SECT, BLDG. 4484 REDSTONE ARSENAL, AL 35898	2
MATERIEL SYSTEMS ANALYSIS ACTV ATTN: DRXSY-MP ABERDEEN PROVING GROUND, MD 21005	1	COMMANDER US ARMY FGN SCIENCE & TECH CTR ATTN: DRXST-SD 220 7TH STREET, N.E. CHARLOTTESVILLE, VA 22901	1

NOTE: PLEASE NOTIFY COMMANDER, ARMAMENT RESEARCH AND DEVELOPMENT CENTER,
US ARMY AMCCOM, ATTN: BENET WEAPONS LABORATORY, SMCAR-CCB-TL,
WATERVLIET, NY 12189-4050, OF ANY ADDRESS CHANGES.

	NO. OF COPIES		NO. OF COPIES
COMMANDER US ARMY LABCOM MATERIALS TECHNOLOGY LAB ATTN: SLCMT-IML WATERTOWN, MA 01272	2	DIRECTOR US NAVAL RESEARCH LAB ATTN: DIR, MECH DIV CODE 26-27, (DOC LIB) WASHINGTON, D.C. 20375	1 1
COMMANDER US ARMY RESEARCH OFFICE ATTN: CHIEF, IPO P.O. BOX 12211 RESEARCH TRIANGLE PARK, NC 27709	1	COMMANDER AIR FORCE ARMAMENT LABORATORY ATTN: AFATL/DLJ AFATL/DLJG EGLIN AFB, FL 32542	1 1
COMMANDER US ARMY HARRY DIAMOND LAB ATTN: TECH LIB 2800 POWDER MILL ROAD ADELPHIA, MD 20783	1	METALS & CERAMICS INFO CTR BATTELLE COLUMBUS LAB 505 KING AVENUE COLUMBUS, OH 43201	1
COMMANDER NAVAL SURFACE WEAPONS CTR ATTN: TECHNICAL LIBRARY CODE X212 DAHLGREN, VA 22448	1		

NOTE: PLEASE NOTIFY COMMANDER, ARMAMENT RESEARCH AND DEVELOPMENT CENTER, US ARMY AMCCOM, ATTN: BENET WEAPONS LABORATORY, SMCAR-CCB-TL, WATERVLIET, NY 12189-4050, OF ANY ADDRESS CHANGES.

END

DTIC

6 - 86